*Paper No. 816. (quote when citing this article)*
Eleventh World Conference on Earthquake Engineering
ISBN: 0 08 042822 3

# STRENGTH AND ENERGY DISSIPATION CHARACTERISTICS OF REINFORCED CONCRETE WALLS UNDER SHEAR FAILURE

P. A. HIDALGO and R. M. JORDAN

Department of Structural and Geotechnical Engineering, Catholic University,
Casilla 306, Correo 22, Santiago, CHILE

## ABSTRACT

The shear strength and the earthquake behavior of reinforced concrete shear walls that exhibit the shear mode of failure are studied. The characteristics of the experimental program consisting in the test of fourteen reinforced concrete, full scale, shear walls under simulated earthquake conditions are described. All the walls had an aspect ratio equal or less than unity, had rectangular cross sections and were designed to fail in shear. The results obtained were used to study the analytical prediction of their shear strength. The energy absorption and dissipation characteristics of eight of the specimens are also analyzed, thus permitting the derivation of an analytical model to represent their hysteretic behavior.

## KEYWORDS

Shear walls; reinforced concrete; shear failure; shear strength; energy dissipation.

## INTRODUCTION

Earthquake-resistant structural systems generally used in reinforced concrete buildings may be one of the following: moment resisting space frames, shear walls, or a combination of both. The use of shear walls is not often in earthquake-prone countries and this fact may explain why moment resisting space frames have attracted so far the attention of the majority of researchers. However, shear wall systems have shown better performance than the space frame systems, as noted many years ago by Fintel (1974) and evidenced by the behavior of Chilean buildings during the March 3, 1985 earthquake.

The lessons learned from the seismic behavior of Chilean buildings show that detailing of reinforced concrete elements to absorb and dissipate energy through the development of ductile flexural behavior, is not the only way to achieve a satisfactory seismic behavior during severe earthquake events. When the total cross section of walls is large enough, i.e. 0.02 to 0.03 times the floor plan area in each direction of seismic resistance for buildings up to 25-story high, flexural yielding of boundary reinforcement of walls is kept at a moderate level in tall buildings and practically does not develop in low-rise buildings. Additionally, shear stresses in the walls are limited to reasonably low values. These facts yield to a satisfactory control of the structural damage, and far more important, to a system where collapse is almost unthinkable. From a conceptual point of view, development of excessive amount of ductility and structural damage is not only prevented because of the considerable lateral strength provided by the shear walls, but also because of the stiffness of the shear wall system. This latter fact is also important to control damage in non-structural

elements. Finally, but not less important, all these benefits may be obtained with methods of design and construction that are much less sophisticated than those required when the survival of a structure under severe earthquake events depends on the development of ductile inelastic behavior in the structural elements.

Nevertheless, the extrapolation of this successful experience to other earthquake-prone countries may not be easy for a number of reasons. Engineering communities have their particular characteristics concerning architectural layouts, building construction skills and cost of workmanship, soil conditions, etc. However, this fact cannot be used to deny significance to the study of the characteristics of seismic behavior of shear wall systems. In the present study, the behavior of walls that exhibit the shear mode of failure is investigated, since many Chilean buildings showed this type of behavior during past severe earthquakes. This is the typical behavior of low-rise buildings but may also develop in taller buildings depending on the geometric characteristics of the wall-spandrel beam structural system. The experimental program presented herein used squat shear walls to force the shear mode of failure under cyclic lateral loads. The discussion of the results is restricted to two aspects of the seismic behavior of walls, namely, the shear strength and the energy absorption and dissipation characteristics of the shear mode of failure.

Most of the limited amount of research published in the past 30 years on the seismic behavior of reinforced concrete shear walls, has addressed two topics: the ultimate shear strength and the criteria to design the walls against shear. The ultimate shear strength has been studied from two different approaches: the derivation of empirical expressions from the results of experimental research programs (Cárdenas and Magura, 1973, Barda *et al.*, 1977, Vallenas *et al.*, 1979, Aktan and Bertero, 1985, Wood, 1989), and the development of rational models based on the basic concepts of structural mechanics (Collins and Mitchell, 1986, Aoyama, 1991). Most of the seismic design provisions found in codes to estimate the ultimate shear strength of walls follow the first of these approaches, and among them, the ACI provisions (ACI Committee 318, 1989) that have been in effect since 1971 are perhaps the most widely used in earthquake-prone countries. The other topic found in the literature is the study of criteria to design against shear. Most of these research efforts have had the objective of avoiding the shear mode of failure in favor of the development of the ductile flexural failure of the walls, like the studies performed by Muto (1965), Paulay *et al.* (1982) and Aktan and Bertero (1985), among others. The research presented herein follows a different approach, i.e. to study the characteristics of the shear mode of failure of shear walls.

## EXPERIMENTAL PROGRAM AND TEST RESULTS

The specimens included in this program were designed with enough boundary vertical reinforcement to develop the shear mode of failure. All specimens were squat walls having aspect ratios $M/Vl_w$ between 0.35 and 1.00, where M is the bending moment at the base of the wall, V the shear force and $l_w$ the length of the wall. Other test parameters were the amount of distributed vertical and horizontal reinforcement. General characteristics of wall specimens are shown in the first seven columns of Table 1. Concrete strength and amounts of reinforcement were selected according to Chilean practice. Wall specimens 3 and 5 have not been included since they were tested under simultaneous axial compression; all the other tests had no axial compression. Due to the reduced thickness of walls, the distributed vertical and horizontal reinforcement were placed in one curtain only. The concrete strength determined the same day of the test varied between 16 MPa (2320 psi) and 20 MPa (2900 psi); yield strength of distributed reinforcement ranged from 320 MPa (46.4 ksi) to 480 MPa (69.6 ksi). The test set-up shown in Fig. 1 was designed to prevent the rotation of both top and bottom ends of the specimen while the horizontal cyclic load is applied at midheight of the wall; reinforced concrete, solid bases were designed at both top and bottom ends to anchor the specimen to the test set-up.

The loading sequence of each specimen consisted of sets of two displacement cycles at a specified displacement amplitude, as shown in Fig. 2. The specified amplitude was gradually increased and followed a sequence that varied according to the aspect ratio. The duration of each cycle was approximately 10 minutes. The test was controlled by a computer that also acquired all the data, but could be stopped at any time to observe the appearance and propagation of cracks, verify instrumentation, etc. Instrumentation was installed in the specimen to measure the horizontal displacement at the top section, rotation of the top

Table 1. Characteristics of wall specimens and test results

| Specimen | $t_w$ (cm) | $l_w$ (cm) | $h_w$ (cm) | $M/(Vl_w)$ | $\rho_h$ (%) | $\rho_v$ (%) | $V_{cr}$ (kN) | $V_u$ (kN) | $\delta_u$ (mm) |
|---|---|---|---|---|---|---|---|---|---|
| 1 | 12 | 100 | 200 | 1.00 | 0.131 | 0.251 | 138.6 | 202.2 | 13.12 |
| 2 | 12 | 100 | 200 | 1.00 | 0.246 | 0.251 | 134.0 | 274.8 | 15.08 |
| 4 | 12 | 100 | 200 | 1.00 | 0.381 | 0.251 | 152.5 | 330.3 | 15.09 |
| 6 | 12 | 130 | 180 | 0.69 | 0.131 | 0.259 | 219.0 | 315.3 | 7.95 |
| 7 | 12 | 130 | 180 | 0.69 | 0.246 | 0.125 | 216.8 | 371.2 | 11.27 |
| 8 | 12 | 130 | 180 | 0.69 | 0.246 | 0.259 | 226.2 | 381.5 | 9.95 |
| 9 | 10 | 130 | 180 | 0.69 | 0.255 | 0.255 | 226.9 | 263.3 | 9.76 |
| 10 | 8 | 130 | 180 | 0.69 | 0.250 | 0.250 | 118.2 | 190.4 | 8.35 |
| 11 | 10 | 140 | 140 | 0.50 | 0.127 | 0.255 | 115.9 | 239.4 | 4.85 |
| 12 | 10 | 140 | 140 | 0.50 | 0.255 | 0.127 | 140.4 | 310.0 | 6.95 |
| 13 | 10 | 140 | 140 | 0.50 | 0.255 | 0.255 | 146.4 | 294.2 | 4.96 |
| 14 | 8 | 170 | 120 | 0.35 | 0.125 | 0.250 | 234.5 | 260.5 | 3.05 |
| 15 | 8 | 170 | 120 | 0.35 | 0.250 | 0.125 | - | 375.1 | 5.07 |
| 16 | 8 | 170 | 120 | 0.35 | 0.250 | 0.250 | 186.1 | 369.2 | 4.48 |

1kN = 0.225 kip; 1 cm = 10 mm = 0.394 in

Table 2. Comparison between experimental results and ACI code predictions

| Specimen | | Experimental Results | | | | ACI 318 Prediction | | | Ratio |
|---|---|---|---|---|---|---|---|---|---|
| N° | $M/(Vl_w)$ | $V_u$ (kN) | $V_s$ (kN) | $V_c$ (kN) | $v_c/\sqrt{f_c'}$ (*) | $V_n$ (kN) | $V_s$ (kN) | $V_c$ (kN) | $V_{n\ ACI}/V_{u\ exp}$ |
| 1 | 1.00 | 202 | 68 | 134 | 0.80 | 197 | 63 | 134 | 0.97 |
| 2 | 1.00 | 275 | 124 | 151 | 0.89 | 256 | 121 | 135 | 0.93 |
| 4 | 1.00 | 330 | 185 | 145 | 0.86 | 322 | 187 | 135 | 0.98 |
| 6 | 0.69 | 315 | 63 | 252 | 1.20 | 231 | 65 | 166 | 0.74 |
| 7 | 0.69 | 371 | 169 | 202 | 0.96 | 351 | 184 | 167 | 0.95 |
| 8 | 0.69 | 382 | 169 | 213 | 1.08 | 341 | 184 | 157 | 0.89 |
| 9 | 0.69 | 263 | 116 | 147 | 0.85 | 262 | 124 | 138 | 1.00 |
| 10 | 0.69 | 190 | 95 | 95 | 0.71 | 204 | 97 | 107 | 1.07 |
| 11 | 0.50 | 240 | 63 | 177 | 0.98 | 209 | 66 | 143 | 0.87 |
| 12 | 0.50 | 310 | 127 | 183 | 0.99 | 280 | 133 | 147 | 0.90 |
| 13 | 0.50 | 294 | 128 | 166 | 0.87 | 286 | 135 | 151 | 0.97 |
| 14 | 0.35 | 261 | 53 | 208 | 1.16 | 206 | 63 | 143 | 0.79 |
| 15 | 0.35 | 375 | 95 | 280 | 1.48 | 278 | 127 | 151 | 0.74 |
| 16 | 0.35 | 369 | 95 | 274 | 1.45 | 277 | 127 | 150 | 0.75 |

(*) $v_c$ and $f_c'$ in kgf/cm$^2$; 1 kgf/cm$^2$ = 0.102 MPa = 14.8 psi; 1kN = 0.225 kip

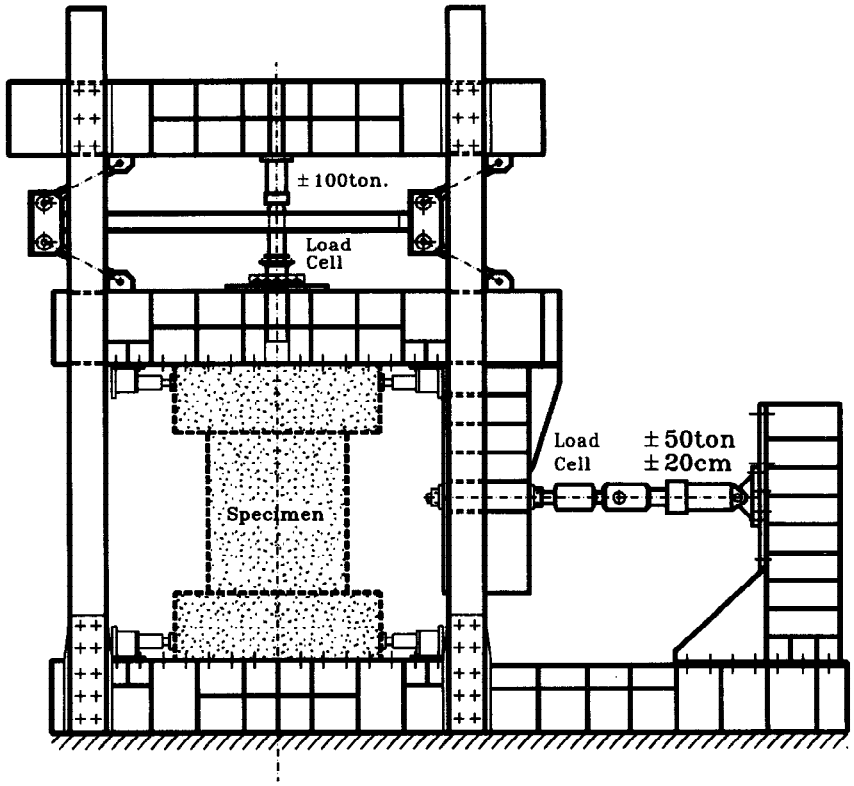


Fig.1 Test set-up

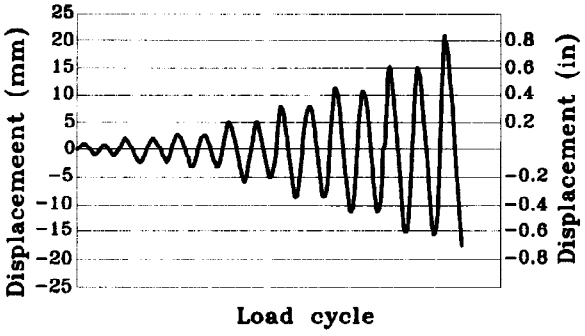


Fig.2 Horizontal displacement history used in tests.

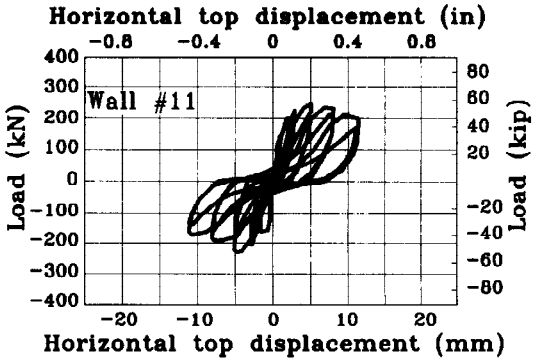


Fig.3 Test results. Hysteresis curves.

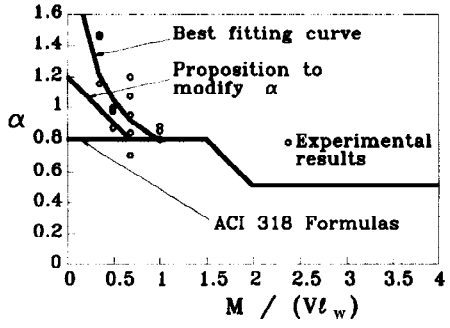


Fig.4 Factor $\alpha$ in ACI code for shear strength of walls.

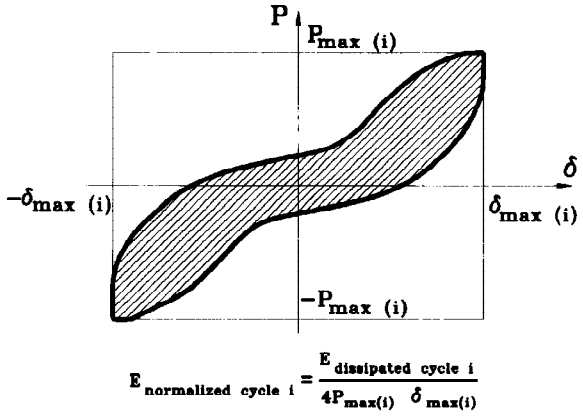


Fig.5 Definition of normalized dissipated energy.

anchorage base, the relative rotation between sections located at a distance of 15 cm (5.91 in) to evaluate the horizontal displacement due to flexure, and the strains at selected locations of the boundary and distributed reinforcement by using strain gages epoxied to the reinforcing bars.

The last three columns of Table 1 show the main results obtained from the tests. The cracking load $V_{cr}$ is the load that produced the first diagonal crack from corner to corner of the specimen; the value indicated in Table 1 is the average value of the cracking loads for both directions of action. Likewise, the value of $V_u$ corresponds to the average value of the maximum shear loads attained during the test in both directions, and $\delta_u$ the average value of the horizontal displacements at the top section corresponding to the maximum loads $V_u$. In all cases, the values that were averaged were quite similar and corresponded to the same or consecutive cycles of the test sequence. The crack widths corresponding to the cracking loads ranged from 0.3 mm (0.0118 in) to 0.6 mm (0.0236 in).

Figure 3 shows the load-displacement hysteresis curves obtained from the test of specimen 11. The displacement is the horizontal displacement measured at the top section of the wall. The behavior shown in Fig. 3 is clearly controlled by the shear mode of failure and is typical of the behavior obtained in the test of all specimens; initial behavior is practically linear-elastic but pinching appears as soon as diagonal cracking develops, reflecting the transition between closing of cracks in one direction and opening of cracks in the opposite direction. All tests were finished when the strength of the specimen had dropped to 75% of the maximum value, approximately.

## STUDY OF SHEAR STRENGTH

The ACI Code (ACI Committee 318, 1989) assumes that ultimate shear strength of reinforced concrete walls may be evaluated by summing the contributions of both concrete ($V_c$) and horizontal reinforcement ($V_s$). The expression for $V_s$ may be derived from basic equilibrium principles, but the contribution of concrete $V_c$ has been empirically obtained from the results of experimental research programs. In the ACI formulas, $V_c$ depends on the ratio $h_w/l_w$, but strictly speaking it depends on the ratio $M/Vl_w$, where M is the maximum value of the bending moment and V is the shear force. The validity of the ACI formulas was examined using the results of the tests of this experimental program as follows.

In the case of specimens 1 to 8 the value of $V_s$ was computed assuming that yielding had been attained in each of the horizontal bars that crossed the main diagonal crack, based on the fact that stress-strain curves of that reinforcement showed a distinctive and rather long yield plateau. In the case of specimens 9 to 16, it was possible to estimate the strains in the horizontal reinforcement from the strain-gages located close to the diagonal crack, and to obtain the corresponding stresses from the stress-strain curves obtained for that reinforcement. Afterwards, the contribution of concrete $V_c$ was estimated by evaluating $V_u - V_s$. The values of $V_s$ and $V_c$ are indicated in Table 2 under the columns labeled "Experimental Results", as well as the ratio $\alpha = v_c/\sqrt{f_c'}$ where $v_c$ and $f_c'$ are used in kgf/cm$^2$; according to ACI formula (21-7) this value should be 0.80 for wall specimens with $M/Vl_w$ equal to or less than 1.5.

Table 2 also shows the estimations of $V_c$, $V_s$ and $V_n = V_s + V_c$ according to ACI formula (21-7) and the ratio between the ACI value for $V_n$ and the experimental strength $V_u$. Several conclusions may be drawn from Tables 1 and 2. First of all, the experimental contribution of concrete $V_c$ is similar for specimens with the same ratio $M/Vl_w$. This value of $V_c$ is close to the cracking load $V_{cr}$ for walls with $M/Vl_w$ equal to or larger than 0.69, which is the accepted hypothesis for reinforced concrete beams, but $V_c$ is different from $V_{cr}$ for walls with smaller values of the ratio $M/Vl_w$. It is clear from Table 2 that ratio $\alpha = v_c/\sqrt{f_c'}$, assumed as 0.80 in the ACI Code, is reasonably close to the experimental values for walls with $M/Vl_w$ equal to or larger than 0.50, but is too conservative for walls with $M/Vl_w$ equal to 0.35. Parameter $\alpha$ has been plotted in Fig. 4 against the aspect ratio $M/Vl_w$, where the conservatism of ACI to estimate $V_c$ for squat walls is clearly shown. Figure 4 also shows the curve that best fits the experimental results and a proposition to linearly increase the value of $\alpha$ from 0.80 for $M/Vl_w = 0.70$ to $\alpha = 1.20$ for $M/Vl_w = 0$.

Table 2 also shows that ACI estimation of $V_s$ is quite good for all wall specimens, except those with $M/Vl_w$

equal to 0.35. In these specimens the height $h_w$ is less than the length $l_w$ and the corner-to-corner diagonal crack forms an angle with the horizontal line that is less than 45°. As the 45° angle of the diagonal crack is one of the hypothesis of the ACI formula, the estimation of $V_s$ may be improved by using the minimum value among $h_w$ and $l_w$ when computing the area $A_{cv}$ and $V_s$ from equation (21-7). If both the modifications for the parameter $\alpha$ and that for evaluating of $V_s$ were used, all the ratios in the last column of Table 2 would fall in the range $1.0 \pm 0.10$.

## MODEL FOR THE HYSTERETIC BEHAVIOR IN THE SHEAR MODE OF FAILURE

When structures or elements do not exhibit a clear yield point, like the behavior of walls under the shear mode of failure, it is not easy to evaluate the displacement ductility ratio. In such a case, it is necessary to go back to the concept that is behind that of ductility, which is the energy absorption and dissipation capacity. The energy dissipated may be evaluated by calculating the area enclosed by the hysteresis loops of the load-displacement curves indicated in Fig. 3. Such calculations were performed for specimens 9 to 16, until the shear strength had dropped to 80% of the maximum strength $V_u$, and showed the energy dissipated decreases with decreasing values of the parameter $M/Vl_w$ and with decreasing amounts of the horizontal reinforcement. However, it is more relevant to compute the "normalized energy dissipated per cycle" by using the definition indicated in Fig. 5. Next, the "average normalized energy dissipated per cycle" may be calculated by dividing the sum of the normalized energy between the cycles defined by the cracking load $V_{cr}$ and the 0.80 $V_u$ load, by the number of cycles developed in between. The last three columns of Table 3 indicate the sum of the normalized energy, the number of cycles involved and the average normalized energy per cycle, respectively. It is surprising to see that numerical values of last column of Table 5 are quite constant with an average value of 0.254. Moreover, it was observed that the normalized energy per cycle shows a small variation between the first cycle, corresponding to $V_{cr}$, and the last cycle, corresponding to the maximum load of 0.80 $V_u$, with average values of 0.20 for the first cycles and 0.27 for the last cycles. These experimental facts may be used to characterize the hysteretic behavior of wall specimens exhibiting the shear mode of failure, by assuming that the average normalized dissipated energy per cycle is constant and equal to 0.25, from the cycle where the first significant diagonal crack develops until the cycle where the strength has dropped to 80 percent of the maximum shear strength.

On the basis of the above experimental fact, a model for the hysteretic behavior of walls failing in shear is presented. This model is composed of two parts: the model of the hysteresis loops, shown in Fig. 6, and the model of the hysteresis envelope, shown in Fig. 7. It can be shown that the model of Fig. 6 may be defined through two parameters only, i.e., $P_{max}$ and $\delta_{max}$, assuming that the normalized dissipated energy, as defined in Fig. 5, is 0.25 and that stiffness $K_2$ is a percentage of stiffness $K_1$; by inspection of the test results, this percentage was taken as 10%. To determine the hysteresis envelope shown in Fig. 7 it is suggested to assume $V_u$ as the value of $V_n$ from the ACI provisions modified as indicated above, and to approximately assume $V_{cr}$ as the contribution of concrete $V_c$. The displacements that define the hysteresis envelope may be assumed as a function of parameter $M/Vl_w$ as follows, where the numerical values have been determined from linear regression of the experimental results.

$$\delta_{cr} = 0.0019 \frac{Mh_w}{Vl_w} \tag{1}$$

$$\delta_u = (0.00185 + 0.0045 \frac{M}{Vl_w}) h_w \tag{2}$$

$$\delta_{u0.80} = 0.016 \frac{Mh_w}{Vl_w} \tag{3}$$

Figure 8 shows a comparison between the proposed model and the actual hysteretic curve for three cycles of the response of specimen 13. The first cycle has been selected just after cracking of the wall, the second at ultimate strength, and the last very close to the ultimate serviceable condition of the wall. The idea is

Table 3. Normalized dissipated energy

| Specimen | $M/Vl_w$ | Sum of normalized energy (%) | Number of cycles involved | Average normal. energy per cycle (%) |
|---|---|---|---|---|
| 9 | 0.69 | 262 | 11.0 | 23.8 |
| 10 | 0.69 | 247 | 10.1 | 24.5 |
| 11 | 0.50 | 260 | 11.1 | 23.4 |
| 12 | 0.50 | 224 | 8.8 | 25.5 |
| 13 | 0.50 | 233 | 8.9 | 26.2 |
| 14 | 0.35 | 214 | 7.6 | 28.2 |
| 15 | 0.35 | 212 | 8.6 | 24.7 |
| 16 | 0.35 | 210 | 7.9 | 26.6 |

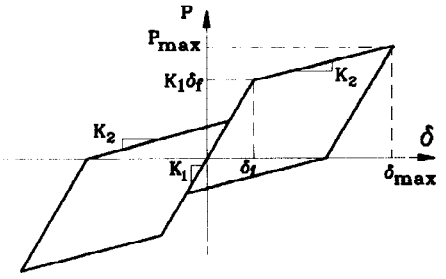


Fig.6 Model for hysteretic cycles.

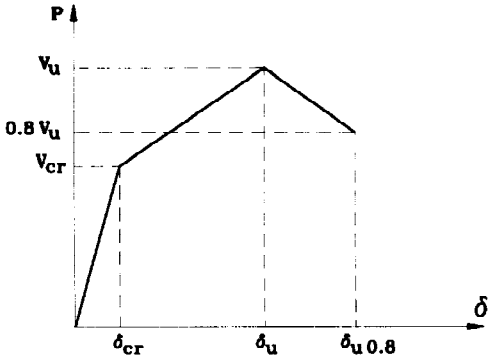


Fig.7 Model for hysteretic envelope.

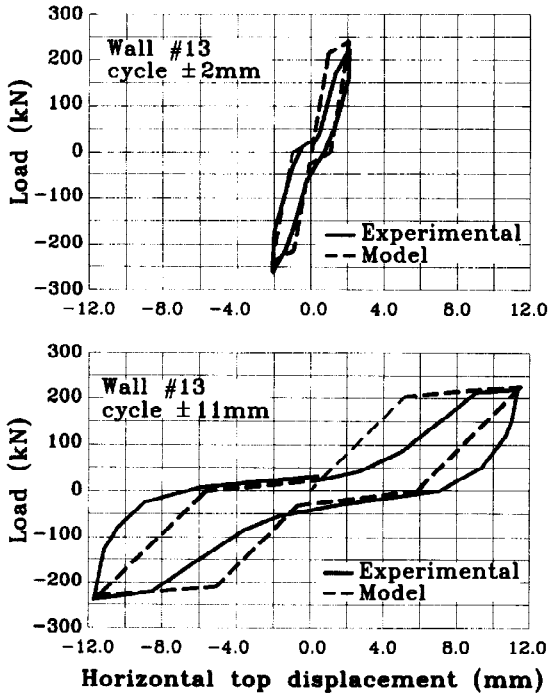


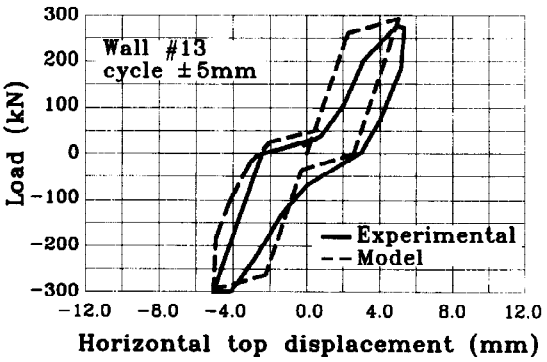


Fig.8 Comparison between model and experimental hysteretic curves.

to check this model against future experimental results and introduce the necessary refinements to obtain an analytical model that may be used to predict the seismic behavior of buildings that exhibit the shear mode of failure.

## CONCLUSIONS

The main conclusions of this study may be summarized as follows:

1. ACI 318 expressions to estimate the shear strength of reinforced concrete shear walls show a reasonably degree of consistency with the results obtained in this test program. Nevertheless, they underestimate the contribution of concrete to the shear strength for walls with aspect ratio $M/Vl_w$ smaller than 0.50, and overestimate the contribution of horizontal reinforcement when the height of the wall is smaller than its length.
2. For walls with low aspect ratio, the contribution of concrete to the ultimate shear strength of walls is different from the shear load that induced the first diagonal shear crack.
3. The energy dissipated by the wall specimens decreases with the aspect ratio of the specimen.
4. The computation of the average normalized energy dissipated per cycle, for cycles after the first diagonal cracking, indicates that this number is nearly constant around 0.25. This fact has allowed to propose an analytical model of the hysteretic behavior of walls that develop the shear mode of failure.

## ACKNOWLEDGEMENTS

The research reported in this paper was funded by the Chilean Superior Council for Technological Development through research projects FONDECYT N° 813/92 and 1930588. The sponsorship of this institution is gratefully acknowledged, as well as the diligent work of graduate student J.L. Larenas and the help and contributions of Professor Carl Lüders of the Catholic University.

## REFERENCES

ACI Committee 318 (1989). "Building Code Requirements for Reinforced Concrete". American Concrete Institute, Detroit, Michigan.

Aktan, A. and Bertero, V. (1985). "RC Structural Walls: Seismic Design for Shear". Journal of Structural Engineering, ASCE, Vol. 111, N°8, 1775-1791.

Aoyama, H. (1991). "Design Philosophy for Shear in Earthquake Resistance in Japan". International Workshop on Concrete in Earthquake, University of Houston, Houston, Texas.

Barda, F., Hanson, J. and Corley W. (1977). "Shear Strength of Low-Rise Walls with Boundary Elements". Reinforced Concrete Structures in Seismic Zones, ACI SP 53-8, 149-201.

Cárdenas, A. and Magura, D. (1973). "Strength of High-Rise Shear Walls - Rectangular Cross Sections". Response of Multistory Concrete Structures to Lateral Forces, ACI SP-36, 119-150.

Collins, M. and Mitchell, D. (1986). "A Rational Approach to Shear Design - The 1984 Canadian Code Provisions". ACI Journal, Title N° 83-80, 925-933.

Fintel, M. (1974). "Ductile Shear Walls in Earthquake Resistant Multistory Buildings". ACI Journal,Title N° 71-19, 296-305.

Muto, K. (1965). "Recent Trends in High-Rise Building Design in Japan". Proceedings Third World Conference on Earthquake Engineering, New Zealand, Vol. 1, 118-147.

Paulay, T., Priestley, M.J.N. and Synge, A.J. (1982). "Ductility in Earthquake Squat Shearwalls". ACI Journal, Title N° 79-26, 257-269.

Vallenas, J., Bertero, V. and Popov, E. (1979). "Hysteretic Behavior of Reinforced Concrete Structural Walls". Report N° UCB/EERC 79/20, University of California, Berkeley, California.

Wood, S. (1989). "Minimum Tensile Reinforcement Requirements in Walls". ACI Structural Journal, Title N° 86-S56, 582-591.